

QSPR correlation for conductivities and viscosities of low-temperature melting ionic liquids

Riccardo Bini^a, Marco Malvaldi^a, William R. Pitner^b and Cinzia Chiappe^{a*}

In order to rationalize the physicochemical behaviour of ionic liquids (ILs), quantitative structure–property relationship (QSPR) models have been derived for the conductivity and viscosity of a class of ILs based on the bis(trifluoromethylsulphonyl)imide anion. Data obtained at two different temperatures were analysed to assess the consistency of the derived relationships. Satisfactory correlations were found for both properties, although the QSPR derived for viscosity was heavily temperature dependent. ILs containing nitrile-functionalized cations could not be inserted into satisfactory QSPR. Copyright © 2008 John Wiley & Sons, Ltd.

Keywords: ionic liquids; conductivity; viscosity; QSPR correlation

INTRODUCTION

Ionic liquids (ILs) are salts that are liquid at ambient temperature and are generally composed of an organic cation (typically, a quaternary ammonium or a functionalized imidazolium cation) and an anion, which is usually inorganic. The study of ILs has experienced huge growth in recent years as a promising field for the development of new environmentally sustainable technologies. The interesting features of ILs include a negligible vapour pressure, excellent and adjustable solvation power for organic, inorganic and polymeric compounds, non-flammability, high thermal and electrochemical stability. These properties make ILs a viable alternative to organic volatile solvents and have stimulated a great deal of interest in the use of ILs in a wide range of applications, including chemical synthesis, separation processes, catalysis and as electrolytic solutions for batteries and for electrodepositions of metals.^[1–7]

Careful choice of the anion–cation combination allows synthesis of ILs with physical and chemical properties tailored to a specific task.^[8] According to Katritzky *et al.*,^[9] there are approximately 10^{18} anion–cation combinations that can lead to useful ILs; therefore, it is necessary to develop and employ predictive computational tools capable of contributing to the design of new ILs with the desired properties.

The target properties of this study were ionic conductivity and viscosity. In solvents designed for organic reactions, viscosity determines the kinetic regime (diffusion-controlled or activation-controlled) and, if the reaction is diffusion-controlled, is a parameter entering directly in the kinetic constant. Even in an activation-controlled regime, however, highly viscous media display a non-negligible dependence of the kinetics from viscosity. Application of Kramers theory^[10] is one methodology for accounting for such effects. It is worth noting that ILs do not fulfil the initial assumptions of Kramers theory, and, thus, a microscopic approach, based on time-dependent response functions, is necessary to quantitatively account for the incoherent mechanical fluctuations which are the molecular origin of viscosity. In addition, viscosity is very important as a physical

property in the application of ILs as raw materials as, for example, lubricants or mechanical dampers.^[11]

Conductivity is also an important feature in a wide range of chemical applications involving batteries or electrodeposition of metals, where ILs are now considered as promising deposition media.^[12] Conductivity and viscosity are related phenomena; Walden observed that for aqueous solutions of electrolytes, the magnitude of the equivalent conductivity is inversely proportional to magnitude of the viscosity.^[13] Much thought has recently focused on the application of the Walden's observation to ILs, which are pure electrolyte systems rather than aqueous solutions. Deviations from the relationship have been used to classify electrolytes as super-ionic, ionic and poorly ionic,^[14] to explore the 'ionicity' of ILs^[15] and to investigate ion-pair formation.^[16]

To test a possible predictive method, we have employed an approach based on descriptors derived from molecular orbital (MO) calculations. Such models based on quantitative structure–property relationship (QSPR) coupled with such kind of descriptors have previously been proposed for the predicting the melting point of ILs.^[8,17–22] Three recent papers have proposed this approach for predicting viscosity and conductivity.^[23,24]

Although a great number of studies on the thermophysical and transport properties of ILs have been published up to now, they cannot be used to build up a consistent and reliable database to be used in order to compare different systems or to perform numerical analysis. This is due to several reasons: experimental

* Correspondence to: C. Chiappe, Dipartimento di Chimica Bioorganica e Biofarmacia, Università di Pisa, via Bonanno 33, 56126 Pisa, Italy.
E-mail: cinziac@farm.unipi.it

a R. Bini, M. Malvaldi, C. Chiappe
Dipartimento di Chimica Bioorganica e Biofarmacia, Università di Pisa, via Bonanno 33, 56126 Pisa, Italy

b W. R. Pitner
Performance and Life Science Chemicals R&D, Merck KGaA, Frankfurter Straße 250, 64293 Darmstadt, Germany

data are given for different systems coming from different sources or are measured under non-equivalent conditions. For example, viscosities are often measured with ordinary viscometers without the possibility to define the shear rate, which are designed for low-viscosity fluids and thus have an unacceptably high experimental uncertainty when used with high-viscosity (and non-Newtonian) ILS. Another source of poor reproducibility is the unknown level of impurities arising from sample preparation and handling (e.g. halides, water), which can strongly affect the transport properties of ILS.^[25,26] Thus, measurements performed in different laboratories on samples prepared with different procedures containing unreported quantities of impurities often do not match an acceptable degree of reproducibility for constructing and testing a model.

In the following, correlations will be presented on a data set collected from ILS synthesized and characterized in the same laboratory, and not taken from literature; only few such studies has currently employed this methodology, and this on a necessarily limited data set.^[21,27]

METHODS

Synthesis and characterization

The synthesis of the ILS used for this research follow well-established protocols.^[28] All chemicals were used as supplied without further purification. The general procedure for IL synthesis was as follows: a haloalkane (1.1 mol) and an organic base (1.0 mol) were combined with 150 ml acetonitrile and stirred under reflux at 80 °C for up to 10 days. The solution was cooled to room temperature and the resulting halide salt was crystallized through the addition of ethyl acetate, isolated by filtration, rinsed with further washings of ethyl acetate and dried under reduced pressure (*ca.* 1 mbar) at 60 °C for 24 h. A portion of the isolated halide salt (0.5 mol) was then dissolved in 150 ml of deionized water, to which was added an aqueous solution of $\text{H}[\text{N}(\text{SO}_2\text{CF}_3)_2]$ (0.6 mol). After mixing the resulting two-phase mixture for 1 h, 100 ml of dichloromethane was added, and the organic and aqueous phases were separated. The organic phase was washed with deionized water and then dried under vacuum to remove both the dichloromethane and residual water to yield the IL.

The identity of each IL was confirmed with ¹H NMR spectroscopy and ESI mass spectroscopy. Halide content was determined by ionic chromatography using a Metrohm system equipped with a model 820 IC separation center, a 819 IC detector and a Metrosepp A Supp 5 column; the eluent was an aqueous mixture containing $3.2 \times 10^{-3} \text{ mol L}^{-1} \text{ Na}_2\text{CO}_3$, $1.0 \times 10^{-3} \text{ mol L}^{-1} \text{ NaHCO}_3$ and 5% acetonitrile. Water content was determined coulometrically using a Metrohm model 831 KF Coulometer with CombiCoulomat fritless Karl–Fischer reagent. All reported viscosity, density, and conductivity values are for ILS containing less than 500 ppm water and less than 100 ppm halide.

Viscosity measurements were performed with an Anton Paar model SVM 3000 Stabinger Viscometer. Conductivity measurements were carried out using a Knick model Konduktometer 703 conductivity meter equipped with a model ZU6985 conductivity cell; the sample cell was placed in a Binder model MK 53 climate control box, which controlled the temperature to ± 0.1 °C. The ILS synthesized, together with values of viscosity, density and conductivity are reported in Table 1.

Calculations

All *ab initio* quantum mechanical calculations have been performed with Gaussian 03.^[29] The cations were optimized at the DFT level with the B3LYP functional. Vibrational frequencies were calculated for all cations using the same level of theory as the optimizations. Partial atomic charges, unless specified otherwise in the description of electrostatic properties, were calculated using the Natural Bond Orbital method as implemented in Gaussian.

The program CODESSA version 2.7.5^[30] was employed to derive correlations between each descriptor and the conductivity and viscosity data in order to derive the QSPRs and to calculate the statistics for the same relationships. For each QSPR the correlation coefficient (*r*), the Fisher significance parameter (*F*), the cross-validated correlation coefficient calculated using a leave-one-out method (R2cv) and the corrected mean square error (*s*2) were determined. CODESSA's heuristic method was used to obtain viscosity and conductivity QSPRs. Before derivation of QSPRs, the method selects descriptors that correlate poorly with the property data, ill-defined descriptors for some compounds and descriptors intercorrelating with other descriptors; these selected descriptors are discarded for the calculations of QSPRs.

CODESSA divides the descriptors into classes: constitutional, topological, geometrical, electrostatic, quantum mechanical and thermodynamic. Of these classes, constitutional, topological and geometrical descriptors are usually not among the best descriptors and their chemical implications appears often unclear, and are unhelpful in the rationalization of the experimental behaviour on the basis of QSPRs. For these reasons, in the following calculations only the electrostatic, quantum mechanical and thermodynamic descriptors have been used. The starting descriptor pool consisted of 250–254 descriptors, depending on the nature of the molecule. With the heuristic method, elimination of ill-defined, inter-correlated and poorly correlated descriptors led to a set of about 120 descriptors.

RESULTS AND DISCUSSION

The properties analysed are viscosity and conductivity of 33 ILS based on imidazolium, pyridium, piperidinium and morpholinium cations, bearing linear alkyl or oxyalkyl chains. Data were collected at two different temperatures (293 and 353 K, respectively), in order to assess if the temperature region at which the correlations are performed can affect the best descriptor set used and the correlations founded. For each data set, we performed correlations for a growing number of descriptors in the range from 1 to 8. Plots of R2 and R2cv values against the number of descriptors, together with analysis of the relative importance of further descriptors in the QSPRs, can provide some indications about the number of descriptors adequate to describe the model.

As a first aspect, all data points pertaining to nitrile-functionalized ILS in the original data set were obvious outliers, falling well outside the 95% confidence limit. This is not surprising: recent reports^[31] have indicated that this class of compounds displays rather peculiar properties (such as extremely high viscosity) independent from the aromatic or aliphatic head group of the cation. To improve the quality of the correlation, all of the data pertaining to the nitrile-functionalized ILS have been discarded from the data set in the actual QSPR calculations presented.

Table 1. ILs studied with relative values of viscosity, density and conductivity at 293 K

Name	Short name	$\eta/\text{mPa s}$	$\rho/\text{g cm}^{-3}$	$\chi/\text{mS cm}^{-1}$
1-Butyl-3-methylimidazolium bis(trifluoromethylsulphonyl)imide	[bmim][Tf ₂ N]	63 572	14 403	3629
1-(2-Hydroxyethyl)-3-methylimidazolium bis(trifluoromethylsulphonyl)imide	[(e2OH)mim][Tf ₂ N]	11 405	15 801	2433
1-(2-Ethoxyethyl)-3-methylimidazolium bis(trifluoromethylsulphonyl)imide	[(eOe)mim][Tf ₂ N]	5612	14 622	3316
1-(Ethoxymethyl)-3-methylimidazolium bis(trifluoromethylsulphonyl)imide	[(eOm)mim][Tf ₂ N]	69 809	15 052	311
1-(2-Methoxyethyl)-3-methylimidazolium bis(trifluoromethylsulphonyl)imide	[(mOe)mim][Tf ₂ N]	58 917	15 096	375
1-(3-Methoxypropyl)-3-methylimidazolium bis(trifluoromethylsulphonyl)imide	[(mOp)mim][Tf ₂ N]	7182	1475	275
1-Propyl-3-methylimidazolium bis(trifluoromethylsulphonyl)imide	[pmim][Tf ₂ N]	56 402	148	4427
1-(3-Hydroxypropyl)-3-methylimidazolium bis(trifluoromethylsulphonyl)imide	[(pOH)mim][Tf ₂ N]	14 158	15 384	1868
1-Pentyl-3-methylimidazolium bis(trifluoromethylsulphonyl)imide	[qmim][Tf ₂ N]	77 734	1407	2308
N-butyl-N-methylmorpholinium bis(trifluoromethylsulphonyl)imide	[bmmo][Tf ₂ N]	80 329	1444	03 042
N-(2-hydroxyethyl)-N-methylmorpholinium bis(trifluoromethylsulphonyl)imide	[(e2OH)mmo][Tf ₂ N]	96 946	15 752	03
N-(ethoxymethyl)-N-methylmorpholinium bis(trifluoromethylsulphonyl)imide	[(eOe)mmo][Tf ₂ N]	37 676	14 578	05 654
N-(2-methoxypropyl)-N-methylmorpholinium bis(trifluoromethylsulphonyl)imide	[(eOm)mmo][Tf ₂ N]	30 307	14 874	07 055
N-(2-methoxyethyl)-N-methylmorpholinium bis(trifluoromethylsulphonyl)imide	[(mOe)mmo][Tf ₂ N]	47 002	15 118	05 318
N-(3-methoxypropyl)-N-methylmorpholinium bis(trifluoromethylsulphonyl)imide	[(mOp)mmo][Tf ₂ N]	77 679	1475	0268
N-(3-hydroxypropyl)-N-methylmorpholinium bis(trifluoromethylsulphonyl)imide	[(pOH)mmo][Tf ₂ N]	18 266	15 378	01 409
N-pentyl-N-methylmorpholinium bis(trifluoromethylsulphonyl)imide	[qmmp][Tf ₂ N]	923 220	1411	0209
1-Butyl-1-methylpiperidinium bis(trifluoromethylsulphonyl)imide	[bmpp][Tf ₂ N]	25 564	1383	08 237
1-(2-Hydroxyethyl)-1-methylpiperidinium bis(trifluoromethylsulphonyl)imide	[(e2OH)mpip][Tf ₂ N]	24 452	1497	09 235
1-(2-Ethoxyethyl)-1-methylpiperidinium bis(trifluoromethylsulphonyl)imide	[(eOe)mpip][Tf ₂ N]	12 626	1398	1428
1-(Ethoxymethyl)-1-methylpiperidinium bis(trifluoromethylsulphonyl)imide	[(eOm)mpip][Tf ₂ N]	11 145	1425	1833
1-(2-Methoxyethyl)-1-methylpiperidinium bis(trifluoromethylsulphonyl)imide	[(mOe)mpip][Tf ₂ N]	14 806	1447	1413
1-(3-Methoxypropyl)-1-methylpiperidinium bis(trifluoromethylsulphonyl)imide	[(mOp)mpip][Tf ₂ N]	22 842	1412	08 073
1-Propyl-1-methylpiperidinium bis(trifluoromethylsulphonyl)imide	[pmpp][Tf ₂ N]	19 9610	1413	1186
1-(3-Hydroxypropyl)-1-methylpiperidinium bis(trifluoromethylsulphonyl)imide	[(pOH)mpip][Tf ₂ N]	45 547	1465	04913
N-butylpyridinium bis(trifluoromethylsulphonyl)imide	[bpyr][Tf ₂ N]	77 081	14 528	2822
N-(2-hydroxyethyl)pyridinium bis(trifluoromethylsulphonyl)imide	[(e2OH)pyr][Tf ₂ N]	145	15 932	1776
N-(2-ethoxyethyl)pyridinium bis(trifluoromethylsulphonyl)imide	[(eOe)pyr][Tf ₂ N]	66 313	14 703	2642
N-(ethoxymethyl)pyridinium bis(trifluoromethylsulphonyl)imide	[(eOm)pyr][Tf ₂ N]	67 023	15 241	343
N-(2-methoxyethyl)pyridinium bis(trifluoromethylsulphonyl)imide	[(mOe)pyr][Tf ₂ N]	72 805	1521	286
N-(3-methoxypropyl)pyridinium bis(trifluoromethylsulphonyl)imide	[(mOp)pyr][Tf ₂ N]	7882	1484	237
N-(3-hydroxypropyl)pyridinium bis(trifluoromethylsulphonyl)imide	[(pOH)pyr][Tf ₂ N]	15 886	15 508	1446

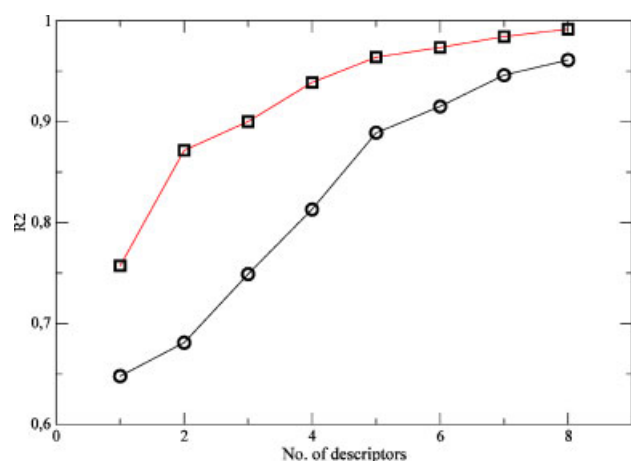


Figure 1. Plot of R^2 at $T = 293$ K (circles) and $T = 353$ K (squares) against the number of descriptors for conductivity QSPR analysis. This figure is available in colour online at www.interscience.wiley.com/journal/poc

Second, for both data sets the quality of QSPR increases with increasing temperature, even when this increase in temperature has the opposite effect on the range and dispersion of experimental data points (which increases for conductivity and decreases for viscosity). Plots of R^2 and R^2_{cv} are reported in Figs. 1 and 2, in support of this conclusion. Such an effect is particularly important for viscosity, and the probable reasons for this will be discussed in detail in the dedicated subsection.

Conductivity

The main correlations of conductivity at 293 and 353 K are reported in Tables 2 and 3, respectively.

The two most statistically significant parameters throughout all correlations for the lower temperature ($T = 293$ K), according to the t -test parameter, are the principal moment of inertia and the maximum net atomic charge for an H atom. This last descriptor is related to the ability of the cation to give stable hydrogen bonds

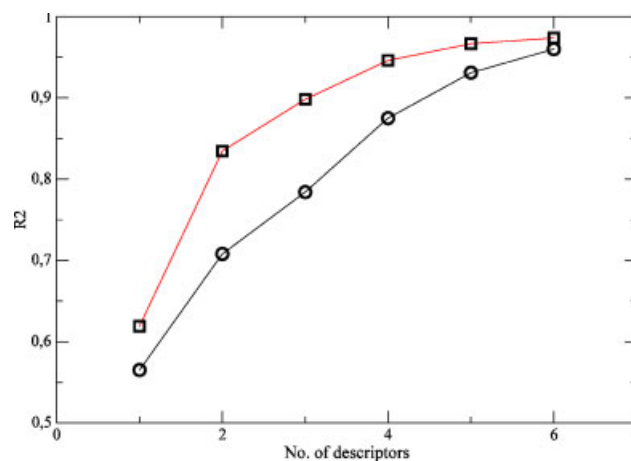


Figure 2. Plot of R^2 at $T = 293$ K (circles) and $T = 353$ K (squares) against the number of descriptors for viscosity QSPR analysis. This figure is available in colour online at www.interscience.wiley.com/journal/poc

Table 2. Correlations of conductivity at $T = 293$ K by the heuristic method

#P	R2	R2cv	F	X + DX	t-Test	Descriptor
1	0.6480	0.5936	49.70	-3.4144e + 00 7.7606e-01 4.8475e + 00 6.8764e - 01	-4.3996 7.0495	Intercept Maximum bond order of a N atom
2	0.6811	0.5712	27.76	4.5991e - 01 5.0582e - 01 2.3965e + 01 3.3883e + 00	0.9092 7.0728	Intercept Principal moment of inertia A
3	0.7489	0.6637	24.85	-3.0029e + 00 1.2492e + 00 -9.4413e + 00 3.7075e + 00	-2.4039 -2.5465	Maximum net charge for a H atom Intercept
4	0.8129	0.6317	26.06	1.6508e + 01 4.8115e + 00 1.5516e + 02 4.6943e + 01	3.4310 3.3053	Maximum electrophilic reactive index for a N atom Minimum 1-electron reactive index for a N atom
				1.2072e + 01 4.4360e + 00 3.2992e - 01 4.0557e - 01	2.7213 0.8135	Minimum bond order of a N atom Intercept
				2.1801e + 01 3.8367e + 00 -5.1829e + 00 1.3031e + 00	5.6821 -3.9775	Principal moment of inertia A Maximum net charge for a H atom
				-5.4994e - 04 1.7011e - 04 1.3261e + 01 4.5474e + 00	-3.2329 2.9161	Lowest normal mode vib. frequency Maximum electrophilic reactive index for a N atom

Table 3. Correlations of conductivity at $T = 353$ K by the heuristic method

#D	R2	R2cv	F	X + DX	t-Test	Descriptor
1	0.7572	0.7158	77.95	1.0332e + 00 1.4100e + 00	0.7328	Intercept
				1.1854e + 02 1.3426e + 01	8.8291	Principal moment of inertia A
2	0.8716	0.8366	81.46	8.7727e + 00 1.1824e + 00	7.4192	Intercept
				2.4313e + 03 1.9978e + 02	12.1694	Principal moment of inertia A
3	0.9000	0.8610	68.97	-1.3310e + 02 2.211e + 01	-6.0178	Maximum partial charge (Qmax)
				9.8919e + 00 1.1527e + 00	8.5816	Intercept
				2.2095e + 03 1.9997e + 02	11.0493	Principal moment of inertia A
				-1.2174e + 02 2.043e + 01	-5.9584	Maximum partial charge (Qmax)
				-7.0256e + 01 2.751e + 01	-2.5538	Maximum 1-electron reactive index for a C atom
4	0.9388	0.9112	84.33	4.1767e + 01 7.7859e + 00	5.3644	Intercept
				1.2168e + 03 2.8636e + 02	4.2491	Principal moment of inertia A
				-1.3417e + 02 2.071e + 01	-6.4785	Maximum partial charge (Qmax)
				5.8154e + 01 1.2471e + 01	4.6633	HA dependent HDSA-1/TMSA
				-2.0287e + 02 4.834e + 01	-4.1961	FPSA-3 fractional PPSA

and, subsequently, to form stable ion pairs that do not contribute to electric conduction. As has been recently argued by Watanabe,^[32,33] the degree of ionicity is of capital importance in the conductivity of ILs and of their mixtures with polar solvents. The principal moment of inertia is related to the length of the substituent alkyl chain, regardless of the kind of functional groups present on the chain. It is not unrealistic that long chains affect the cation's ability to coordinate anions and, therefore, to form ionic pairs of partially 'correlated' anions and cations.^[34] The correlation chart for conductivity at 293 K in the four-descriptors model, which was judged to be satisfying, is reported in Fig. 3.

It is notable that the correlations found for the higher temperature are essentially of the same nature, and that the two main contributions to the correlations are from the same descriptors reported for the data sets related to 293 K. This is equivalent to saying that the analysis of conductivity gives reliable correlations regardless of temperature. The correlation for conductivity at 353 K in the three-descriptors model (Fig. 4) is nevertheless much more satisfying than its four-descriptors counterpart at lower temperatures, displaying an $R^2 = 0.900$

which is quite higher than the value of $R^2 = 0.8174$ obtained with four-descriptors model at lower temperature.

Viscosity

The main correlations of viscosity at 293 and 353 K are reported in Tables 4 and 5, respectively. Here, as in the conductivity analysis, the quality of correlation improves with increased temperature. When the results obtained at the two different temperatures are compared, the important descriptors and correlations obtained in this analysis differ even qualitatively; this is significantly different from the case for conductivity, where the correlating factors were essentially of the same nature.

At the lower temperature (293 K), the most important descriptor appears to be the fractional negative surface area FNSA-3 Fractional PNSA (PNSA-3/TMSA) [Quantum-Chemical PC] and the maximum 1-electron reactive index for a C atom. The first descriptor is a measurement of the negatively charged surface area accessible to the surrounding molecules, while the second is a Fukui function designed specifically to describe chemical

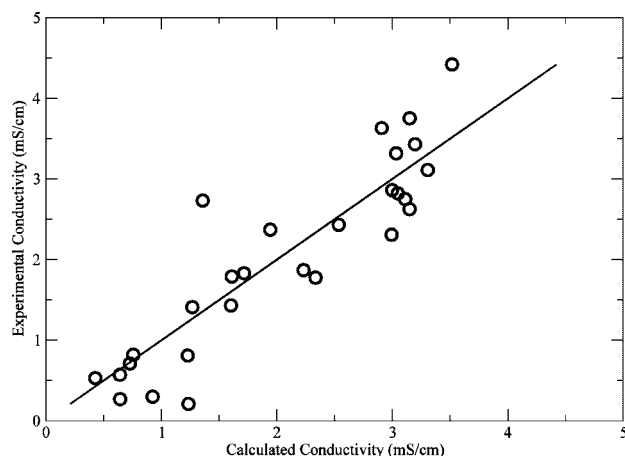
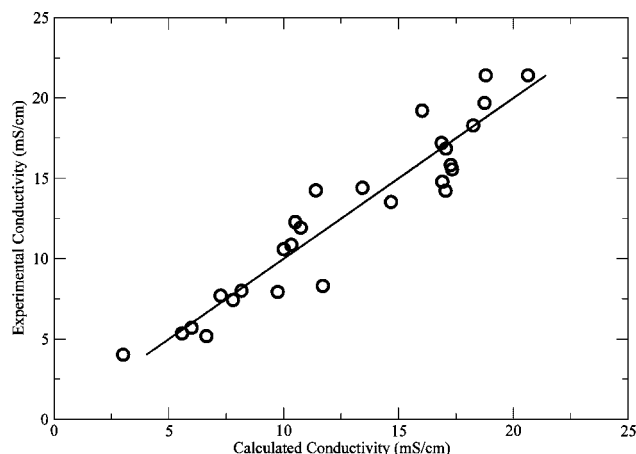
**Figure 3.** Calculated *versus* experimental conductivities at 293 K in the four-descriptors model**Figure 4.** Calculated *versus* experimental conductivities at 353 K in the three-descriptors model

Table 4. Correlations of viscosity at $T = 293$ K by the heuristic method

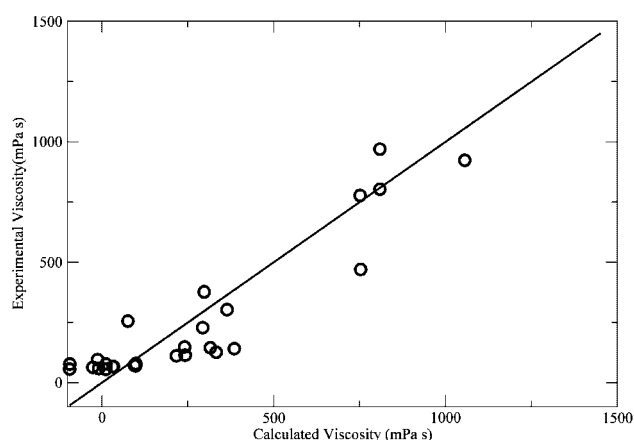
#D	R ²	R ² _{cv}	F	X + DX	t-Test	Descriptor
1	0.5652	0.4107	35.10	-2.1524e + 03 4.1658e + 02 2.9054e + 01 4.9039e + 00	-5.1669 5.9247	Intercept DPSA-3 difference in CPSAs
2	0.7081	0.5870	31.54	7.8235e + 01 8.9379e + 01 -2.2911e + 04 3.0480e + 03 -1.5355e + 03 2.2089e + 02	0.8753 -7.5168 -6.9517	Intercept Avg. nucleophilic reactive index for a O atom Minimum net charge for a O atom
3	0.7842	0.6352	30.29	2.0173e + 03 7.6003e + 02 -1.2457e + 04 2.0231e + 03 1.3351e + 04 2.6852e + 03 -2.1173e + 03 7.0137e + 02	2.6542 -6.1574 4.9721 -3.0188	Intercept FNSA-3 fractional PNSA Maximum 1-electron reactive index for a C atom No. of occ. electronic levels/# of atoms
4	0.8755	0.7647	42.18	-7.1852e + 01 2.9694e + 02 -1.4507e + 04 1.6351e + 03 1.0005e + 04 2.2353e + 03 2.9155e + 02 6.3130e + 01 -3.7319e - 01 8.7371e - 02	-0.2420 -8.8726 4.4759 4.6182 -4.2714	Intercept FNSA-3 fractional PNSA Maximum 1-electron reactive index for a C atom FPSA-2 fractional PPSA Highest normal mode vib. frequency

Table 5. Correlations of viscosity at $T = 353$ K by the heuristic method

#D	R ²	R ² _{cv}	F	X + DX	t-Test	Descriptor
1	0.6191	0.5478	43.88	-4.5057e + 01 9.4166e + 00 7.3432e - 01 1.1085e - 01	-4.7849 6.6245	Intercept DPSA-3 difference in CPSAs
2	0.8345	0.7665	65.54	1.4347e + 01 2.5491e + 00 -1.9461e + 02 2.4518e + 01 -4.1512e + 01 6.2565e + 00	5.6281 -7.9376 -6.6351	Intercept Maximum electrophilic reactive index for a N atom FNSA-2 fractional PNSA
3	0.8982	0.8577	73.49	4.1532e + 01 6.5614e + 00 -1.7823e + 02 2.011e + 01 -7.9424e - 01 8.8380e - 02 -1.7107e + 01 4.073e + 00	6.3297 -8.8623 -8.9867 -4.1991	Intercept Maximum electrophilic reactive index for a N atom PNSA-3 atomic charge weighted PNSA Maximum atomic orbital electronic population
4	0.9460	0.9287	105.1	5.5026e + 01 5.8181e + 00 -1.6570e + 02 1.5039e + 01 -1.2079e + 00 1.0245e - 01 -1.2950e + 02 2.0614e + 01 -7.1295e - 03 1.4367e - 03	9.4577 -11.017 -11.790 -6.2821 -4.9626	Intercept Maximum electrophilic reactive index for a N atom PNSA-3 atomic charge weighted PNSA Polarity parameter (Q _{max} -Q _{min}) Highest normal mode vib. frequency

reactions; both these descriptors can be thought to account for cation–anion interactions. Since the mobility (and thus the viscosity) of an IL is ruled by a slow ion-exchange mechanism,^[34] which is dependent on the interaction strength, the presence of such descriptors appears physically reasonable. Nevertheless, the correlation obtained (Fig. 5) is rather poor: although for the four-descriptor model the R² is satisfying (0.8755), a visual inspection of the correlation chart reveals an unsatisfactory correlation, particularly in the low-viscosity area. A possible explanation for this may be the inhomogeneous distribution of viscosity values in the data set, as a consequence of the fact that morpholinium-based ILs display a viscosity quite higher (about 1 order of magnitude) with respect to the other ILs of the data set. As appears by inspection of Fig. 5, the data set is somewhat spreaded in two regions of low (non-morpholinium) and high (morpholinium) viscosity. The correlation obtained thus matches these two macroregions with different viscosity values, but fails in describing in detail the behaviour of viscosity.

It is nevertheless known that the modelling of viscosity through a descriptor-based QSPR is usually a hard work, and that often this

**Figure 5.** Calculated versus experimental viscosities at 293 K in the four-descriptors model

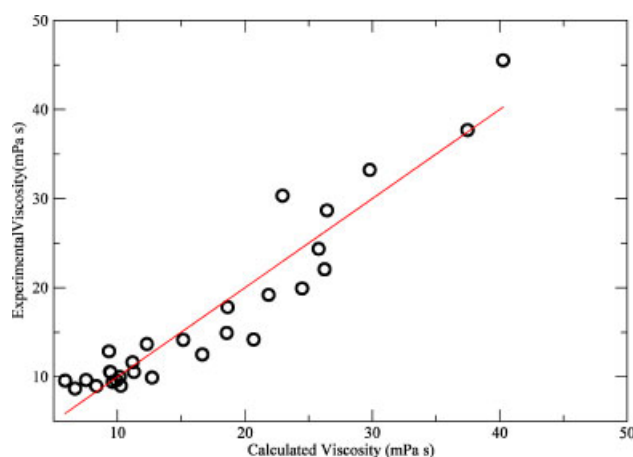


Figure 6. Calculated versus experimental viscosities at 353 K in the three-descriptors model. This figure is available in colour online at www.interscience.wiley.com/journal/poc

property shows nonlinear behaviour. Actually, elimination of the six highest viscosity data points and analysis of the subsequently reduced data set gave qualitatively similar results: this indicates that the inhomogeneity of data set may not be the only factor affecting the quality of the obtained relationship.

A much better correlation set is obtained at the higher temperature (353 K); here, the most important descriptors in all the correlation sets are the FNSA-3 Fractional PNSA (PNSA-3/TMSA) [Quantum-Chemical PC] and the maximum electrophilic reactivity index for a N atom (Fig. 6). As with the former, we interpreted these two descriptors as a measure of the strength of the cation–anion interaction; we note, however, that the descriptors obtained are different from the ones given by the analysis of the lower temperature data. The quality of the correlation obtained here is satisfying; with a three-descriptor model (one less descriptor than for the lower temperature), the R^2 obtained is 0.8982 and the quality of the fit is visually convincing.

A possible reason for the striking difference between the two temperatures may be the fact that complex fluids near to the super-cooling regime or glass-transition temperature often exhibit non-Newtonian behaviour; that is, the viscosity is a function of the shear rate at which it is measured; some ILs have been found to display such behaviour.^[35] As a consequence, comparing the viscosity of a Newtonian and of a non-Newtonian liquid measured at the same shear rate may be seen as comparing two different properties, since the mobility of supercooled and simple liquids is ruled by different phenomena. Comparison of data acquired at elevated temperatures may thus act to eliminate or reduce such differences.

CONCLUSIONS

We have presented QSPR for the conductivity and viscosity of a class of ILs specifically designed for electrochemical applications. Satisfactory correlations have been obtained after elimination from the data set of the data pertaining to nitrile-functionalized cations, which probably exhibit specific interactions not captured by the set of descriptors selected. All the correlations improved when calculated with the data measured at the higher temperature. With respect to viscosity, qualitatively different

correlations were found between the analyses at two different temperatures. The origin of such discrepancies cannot be assessed definitely: we note, however, that the non-Newtonian behaviour of some ILs at room temperature is expected to contribute. Viscosity and conductivity, although correlated in their molecular origin, are described with different accuracy; while conductivity turns out to be a property which is well described by a QSPR approach, viscosity appears to be quite more difficult to rationalize. We have to keep in mind, however, that viscosity is generally speaking a quite difficult property to be modelled or predicted. The problems encountered here in modelling the viscosity behaviour by the QSPR approach are then not surprising.

In this sense, due to the very nature of the properties that are modelled, some bulk properties are efficiently described by QSPR approach in molecular and ILs, while for other properties (typically transport properties) there is room for considerable improvement.

The most important descriptors founded in correlation of both properties are, in principle, a measurement of interaction between ions; this appears physically sound, as the mobility and ability to transport electric charge are intimately connected to the degree of ionic association and the interaction potentials between ions.

From our results, and the studies already presented in the literature, it is our opinion that such numerical approach can find its application in discriminating amongst different classes of ILs (e.g. imidazolium, pyridinium) or to optimize and modulate properties among the same class; nevertheless, its power as a general predictive tool for the whole set of possible ILs appears to be questionable, on the basis of the complexity of correlations obtained for the large and heterogeneous data sets found in the literature.

As explained in the text, we utilized only general electrostatic, thermodynamic, and quantum-chemical descriptors. A possible way to improve the reliability and predictive power of QSPR methods, when applied to ILs, may be to design and test new kind of dedicated descriptors on the basis of what suggested from experiments and chemical knowledge.

As a final remark, we stress that it is common practice to collect experimental data sets for the physico-chemical properties of ILs from reviews or collection of articles, thus obtaining a data set of properties measured in different conditions on ILs synthesized with differing and often unknown degrees of purity. As already stressed in the Section Introduction, it is known that properties of ILs depend heavily on the degree of purity which cannot always be easily controlled. The measured properties for the same IL can thus vary to a non-negligible extent if measured in different situations: we note, as an example, that the values found in the literature for the viscosity of [bmim][Tf₂N] (52 mPa s^[36] and 57.6 mPa s^[37]) differs noticeably (17 and 11%) from the one measured by us (64 mPa s) at nominally the same conditions. It is therefore advisable to perform correlations on data sets obtained under the same conditions, since experimental variation aspect can deeply affect the results.

REFERENCES

- [1] R. A. Sheldon, *Green Chem.* **2005**, 7, 267–278.
- [2] T. Welton, *Chem. Rev.* **1999**, 99, 2071–2084.
- [3] C. L. Hussey, *Pure Appl. Chem.* **1988**, 60, 1786–1792.

- [4] A. Heintz, *J. Chem. Thermodyn.* **2005**, 37, 525–536.
- [5] K. R. Seddon, *J. Chem. Technol. Biotechnol.* **1997**, 68, 351–356.
- [6] D. R. McFarlane, J. Sun, J. Golding, P. Meakin, M. Forsyth, *Electrochem. Acta* **2000**, 45, 1271–1278.
- [7] L. Düran Pachón, C. J. Elsevier, G. Rothenberg, *Adv. Synth. Catal.* **2006**, 348, 1705–1710.
- [8] C. Chiappe, D. Pieraccini, *J. Phys. Org. Chem.* **2005**, 18, 275–287.
- [9] A. R. Katritzky, R. Jain, A. Lomaka, R. Petrukhin, M. Karelson, A. E. Visser, R. D. Rogers, *J. Chem. Inf. Comp. Sci.* **2002**, 42, 225–231.
- [10] H. A. Kramers, *Physica* **1940**, 7, 284–304.
- [11] C. Reichardt, *Solvents and Solvent Effects in Organic Chemistry*, (3rd edn) Wiley-VCH Verlag GmbH & Co. KGaA: Weinheim **2003**, Print ISBN: 9783527306183 Online ISBN: 9783527601790.
- [12] R. Bomparola, S. Caporali, A. Lavacchi, U. Bardi, *Surf. Coat. Technol.* **2007**, 201, 9485–9490.
- [13] P. Walden, *Z. Phys. Chem.* **1906**, 55, 207–249.
- [14] W. Xu, E. I. Cooper, C. A. Angell, *J. Phys. Chem. B* **2003**, 107, 6170–6178.
- [15] H. Tokuda, K. Hayamizu, K. Ishii, M. A. B. H. Susan, M. Watanabe, *J. Phys. Chem. B* **2004**, 108, 16593–16600.
- [16] K. J. Fraser, E. I. Izgorodina, M. Forsyth, J. L. Scott, D. R. MacFarlane, *Chem. Commun.* **2007**, 3817–3819.
- [17] A. R. Katritzky, R. Jain, A. Lomaka, R. Petrukhin, M. Karelson, A. E. Visser, R. D. Rogers, *J. Chem. Inf. Comp. Sci.* **2002**, 42, 71–74.
- [18] D. Eike, J. Brennecke, E. Maginn, *Green Chem.* **2003**, 5, 323–328.
- [19] G. Carrera, J. Aires-de-Sousa, *Green Chem.* **2005**, 7, 20–27.
- [20] A. Varnek, N. Kireeva, I. V. Tetko, I. I. Baskin, V. P. Solov'ev, *J. Chem. Inf. Model.* **2007**, 47, 111–1122.
- [21] S. Trohalaki, R. Patcher, G. W. Drake, T. Hawkins, *Energy Fuels* **2005**, 19, 279–284.
- [22] I. Lopez-Martin, E. Burello, P. N. Davey, K. R. Seddon, G. Rothenberg, *ChemPhysChem* **2007**, 8, 690–695.
- [23] H. Matsuda, H. Yamamoto, K. Kurihara, K. Tochigi, *Fluid Phase Equilib.* **2007**, 261, 434–443.
- [24] H. Yamamoto, K. Tochigi, *J. Phys. Chem. C* **2007**, 111, 15989–15994.
- [25] J. A. Widegren, A. Laesecke, J. W. Magee, *Chem. Commun.* **2005**, 1610–1612.
- [26] K. R. Seddon, A. Stark, M. J. Torres, *Pure Appl. Chem.* **2000**, 72, 2275–2287.
- [27] J. M. Slattery, C. Daguene, P. J. Dyson, T. J. S. Schubert, I. Krossing, *J. Am. Chem. Soc.* **2006**, 128, 13427–13434.
- [28] C. M. Gordon, M. J. Muldoon, in *Ionic Liquids in Synthesis*, 2nd edn (Ed.: P. Wasserscheid, T. Welton), Wiley-VCH Verlags GmbH & Co. KGaA, Weinheim, **2008**, pp. 7–25.
- [29] Gaussian 03, Revision C.01, M. J. Frisch, G. W. Trucks, H. B. Schlegel, G. E. Scuseria, M. A. Robb, J. R. Cheeseman, J. A. Montgomery, Jr., T. Vreven, K. N. Kudin, J. C. Burant, J. M. Millam, S. S. Iyengar, J. Tomasi, V. Barone, B. Mennucci, M. Cossi, G. Scalmani, N. Rega, G. A. Petersson, H. Nakatsuji, M. Hada, M. Ehara, K. Toyota, R. Fukuda, J. Hasegawa, M. Ishida, T. Nakajima, Y. Honda, O. Kitao, H. Nakai, M. Klene, X. Li, J. E. Knox, H. P. Hratchian, J. B. Cross, C. Adamo, J. Jaramillo, R. Gomperts, R. E. Stratmann, O. Yazyev, A. J. Austin, R. Cammi, C. Pomelli, J. W. Ochterski, P. Y. Ayala, K. Morokuma, G. A. Voth, P. Salvador, J. J. Dannenberg, V. G. Zakrzewski, S. Dapprich, A. D. Daniels, M. C. Strain, O. Farkas, D. K. Malick, A. D. Rabuck, K. Raghavachari, J. B. Foresman, J. V. Ortiz, Q. Cui, A. G. Baboul, S. Clifford, J. Cioslowski, B. B. Stefanov, G. Liu, A. Liashenko, P. Piskorz, I. Komaromi, R. L. Martin, D. J. Fox, T. Keith, M. A. Al-Laham, C. Y. Peng, A. Nanayakkara, M. Challacombe, P. M. W. Gill, B. Johnson, W. Chen, M. W. Wong, C. Gonzalez, J. A. Pople, Gaussian, Inc., Wallingford CT, **2004**.
- [30] A. R. Katritzky, V. S. Lobanov, M. Karelson, CODESSA Reference Manual. Version 2.0, University of Florida, **1996**.
- [31] J. M. Slattery, C. Daguene, P. J. Dyson, T. J. S. Schubert, I. Krossing, *Angew. Chem. Int. Ed.* **2007**, 46, 5384–5388.
- [32] H. Tokuda, S. J. Baek, M. Watanabe, *Electrochemistry* **2005**, 73, 620–622.
- [33] H. Tokuda, K. Hayamizu, K. Ishii, M. A. B. H. Susan, M. Watanabe, *J. Phys. Chem. B* **2005**, 109, 6103–6110.
- [34] T. I. Morrow, E. J. Maginn, *J. Phys. Chem. B* **2002**, 106, 12807–12813.
- [35] (Ed.: P. Wasserscheid, T. Welton). *Ionic Liquids in Synthesis* (2nd edn) Wiley-VCH Verlags GmbH & Co. KGaA, Weinheim, **2008**, pp. 7–25.
- [36] T. S. Handy, *Curr. Org. Chem.* **2005**, 9, 959–988.
- [37] S. Zhang, N. Sun, X. He, X. Lu, X. Zhang, *J. Phys. Chem. Ref. Data* **2006**, 35, 1475–1517.